EARTH SURFACE PROCESSES AND LANDFORMS
Earth Surf. Process. Landforms (2020)

Published online in Wiley Online Library
(wileyonlinelibrary.com) DOI: 10.1002/esp.5006

State of Science

Limits to scale invariance in alluvial rivers

Rob Ferguson*
Department of Geography, Durham University, Durham DH1 3LE, UK

Received 30 July 2020; Revised 14 September 2020; Accepted 14 September 2020

*Correspondence to: Rob Ferguson, Department of Geography, Durham University, Durham DH1 3LE, UK. E-mail: r.i.ferguson@durham.ac.uk

ESPL
Earth Surface Processes and Landforms

ABSTRACT: Assumptions about fluvial processes and process–form relations are made in general models and in many site-specific applications. Many standard assumptions about reach-scale flow resistance, bed-material entrainment thresholds and transport rates, and downstream hydraulic geometry involve one or other of two types of scale invariance: a parameter (e.g. critical Shields number) has the same value in all rivers, or doubling one variable causes a fixed proportional change in another variable in all circumstances (e.g. power-law hydraulic geometry). However, rivers vary greatly in size, gradient, and bed material, and many geomorphologists regard particular types of river as distinctive. This review examines the tension between universal scaling assumptions and perceived distinctions between different types of river. It identifies limits to scale invariance and departures from simple scaling, and illustrates them using large data sets spanning a wide range of conditions. Scaling considerations and data analysis support the commonly made distinction between coarse-bed and fine-bed reaches, whose different transport regimes can be traced to the different settling-velocity scalings for coarse and fine grains. They also help identify two end-member sub-types: steep shallow coarse-bed 'torrents' with distinctive flow-resistance scaling and increased entrainment threshold, and very large, low-gradient 'mega rivers' with predominantly suspended load, subdued secondary circulation, and extensive backwater conditions. © 2020 The Authors. Earth Surface Processes and Landforms published by John Wiley & Sons Ltd

KEYWORDS: gravel-bed rivers; sand-bed rivers; scale invariance; flow resistance; entrainment threshold; settling velocity; torrents; mega rivers

Introduction

Individual reaches of alluvial river channels vary greatly in size, discharge, gradient, and sediment calibre. Bankfull width is less than 1 m in some first-order tributaries but over 10 km in multi-channel reaches of major lowland rivers. The range of bankfull discharge is greater still, from <0.1 to $>100\,000$ m^3 s^{-1}. Channel slope is as low as 1×10^{-5} (1 cm drop per river kilometre) in parts of the Amazon basin but more than 0.1 (100 m km^{-1}) in the steepest mountain torrents. The median diameter (D_{50}) of river-bed material ranges from 0.03 mm in some rivers with beds of silt and fine sand to >1 m in some boulder-filled mountain torrents. This immense variety of conditions is to be expected as runoff in vast numbers of tiny headwater tributaries – some steep, others not, depending on the terrain – joins into fewer and fewer, but progressively larger, channels farther towards the sea. These larger rivers typically have lower gradients, partly through the influence of base level, and they generally have finer bed material as a consequence of abrasion and size-selective transport, but these are only broad tendencies that are heavily blurred by the contingencies of topographical, geological, and climatic setting and history. For any given slope, grain size, or bankfull discharge, there is a wide (one to two orders of magnitude) range of possible values of the other two variables.

Any individual reach, wherever positioned within this continuum of river character, is either in or adjusting towards a multi-year balance between transport capacity (which depends on all three of slope, discharge, and grain size) and bed-material sediment supply (for which D_{50} is often regarded as an inverse proxy). There is a long history of attempts by geomorphologists and other river scientists to describe and predict equilibrium configurations, using both theoretical and empirical approaches and sometimes also stochastic or teleological considerations (Benson, 2020). It is increasingly recognized that many reaches are not in equilibrium but adjusting to environmental or anthropogenic changes (Church and Ferguson, 2015), so there is growing interest in predicting transient response as well as equilibrium. In either case the dominant paradigm in recent decades has been physics-compatible theory using quantitative representations of flow and transport processes. General models often involve invariances and simple scaling laws that are assumed valid for many or all rivers; conversely, general scaling rules taken from the literature are used in practical applications at specific sites that vary greatly in character. In this paper I examine whether there are limits to some of these assumptions, and to what extent departures from simple scaling help explain why some types of river appear to be distinctive.

Some aspects of river morphology are scale-invariant in the sense of geometric similarity. Small and large meanders and braids look much the same on maps or satellite imagery because bend and bar wavelengths are directly proportional to channel width (Inglis, 1947; Leopold and Wolman, 1960; Kleinhans *et al.*, 2015) and the length-to-width ratio of mid-channel bars does not vary systematically with scale (Smith *et al.*, 2005). Another type of scale invariance exists when two variables are related in such a way that a given proportional change in one variable (e.g. its value is doubled) is always associated with a fixed proportional change in the other, no matter what absolute values are involved. Power laws and logarithmic or exponential functions have this property. A well-known fluvial example is that channel width and mean depth appear to follow simple power-law relations with bankfull discharge over the full range from laboratory channels and irrigation canals to the largest continent-draining rivers (Lacey, 1930; Leopold and Maddock, 1953; Eaton, 2013).

Invariances and simple scaling laws also feature in the process assumptions underlying many models of channel regime and the evolution of specific features such as bars and bends. The most commonly used flow resistance relation for channels of all sizes and types (the Manning equation) is a power law, and many morphodynamic models assume an invariant value of Manning's n or some other friction factor. The threshold of bed-sediment motion is widely regarded as a fixed value of non-dimensional shear stress (Shields number) irrespective of D_{50} and other river characteristics. Bed-material transport is often modelled by a relation between non-dimensional variables based on transport rate (Einstein's Φ) and shear stress (Shields number again), with differences in slope, discharge, and grain size subsumed into these variables, and the relation is often assumed to be a simple power law.

Simple scaling relations and invariances imply that rivers can be regarded as models of one another, whether they are small or large, steep or almost flat, and have coarse beds or fine. At first sight this is reasonable: no river is so tiny or huge that Newtonian physics has to be replaced by quantum mechanics or general relativity, and it is accepted that dimensionally consistent versions of process relations for rivers on Earth can be used to make inferences about the origins of channels on Mars (e.g. Kleinhans, 2005). However, the existence of sub-literatures for different types of river suggests that geomorphologists do not view rivers as all essentially the same. Bedrock rivers convey water and sediment, just like alluvial rivers, but they have a literature of their own because channel change occurs in very different ways and much more slowly. Within the alluvial category it has sometimes been suggested that rivers in particular climate zones are distinctive (e.g. Tooth, 2000; Latrubesse *et al.*, 2005), and a distinction is commonly made between sand-bed and gravel-bed rivers on the grounds that their sediment transport regimes are fundamentally different (Howard, 1980; Dade and Friend, 1998; Church, 2006). This distinction is supported by the widespread occurrence of abrupt downstream transitions from gravel to sand bed (Yatsu, 1957; Smith and Ferguson, 1995) and the apparent scarcity of reaches with D_{50} in the 1–10mm range (Shaw and Kellerhals, 1982; Dunne and Jerolmack, 2018). There is also a thriving sub-literature on steep channels with cobble/boulder beds (e.g. Palucis and Lamb, 2017). These often have a distinctive morphology (Montgomery and Buffington, 1997; Church, 2006), and it has become recognized that standard equations describing flow and bedload transport in lower-gradient rivers do not work well in steep channels (e.g. Rickenmann, 2001; Ferguson, 2007; Nitsche *et al.*, 2011, 2012). Finally, some geomorphologists have argued that very large ('mega') rivers are distinctive in morphology and possibly also in process terms (Latrubesse, 2008; Ashworth and Lewin, 2012; Nicholas, 2013).

Can the use of scale-invariant process equations and process–form relations be reconciled with recognition of distinctive types of alluvial river at the reach scale? Physicists working at the nanometre scale recognize that even though the same physical equations apply as at larger scales, the relative importance of individual forces is different (Jones, 2004, p. 55). Might such differences be a factor in the alleged distinctiveness of mega-rivers, or those with particularly fine or coarse beds? Alternatively, if process relations and process–form links do depart from scale invariance in particular parts of the continuum of river size, slope, and bed D_{50}, does this help explain the distinctions that field geomorphologists perceive and the typologies they have developed?

My approach to these questions is to examine critically the various simple scaling laws and invariances that have been proposed for the reach-scale hydraulics of rivers, the transport of bed material, and the relations between these and bankfull channel dimensions. I do this with reference to the published literature and by looking at what is shown by the most comprehensive and wide-ranging data sets I can find. Most of the discussion of flow and sediment transport applies to both bedrock and alluvial rivers, but when testing scale relations against measurements I consider only alluvial reaches for lack of data from bedrock channels. I treat 'scale' in a broad sense, considering not just whether simple scaling laws and invariances are valid for channels of all sizes but also whether they hold over the full range of channel gradient and for all calibres of bed sediment. The section on morphology considers only simple scaling relations with discharge and grain size; it is not meant to be a review of the many papers attempting to explain or predict different aspects of channel morphology and morphodynamics.

The last part of the paper summarizes the messages of the three main sections and discusses what they imply about the distinctiveness of particular types of rivers. I show that departures from scale invariance exist in all aspects of river hydraulics, bed-material transport, and regime, although some simple scalings are acceptable over a wide range of conditions. Scaling considerations using reach-scale variables support a distinction between coarse-bed and fine-bed rivers, but do not explain why transitional reaches are infrequent; this requires consideration of mixed grain sizes. Departures from simple scaling also become apparent in very steep coarse-bed channels (torrents) and in very large fine-bed channels (mega rivers). These are distinctive extreme cases of the two main river types but are transitional to them rather than separated by a threshold.

Limits to scale invariance: bulk hydraulics

The conservation of fluid mass and momentum in any river, whatever its size and other characteristics, is described by the Navier–Stokes equations or their simplified time-averaged, time- and depth-averaged, and time- and width-averaged versions. But river flow is affected by two external forces: gravity and friction. These forces vary between reaches depending on channel slope and roughness, and also over time as water discharge fluctuates. Frictional resistance is one of at least three ways in which scale effects are apparent in river flow. The other two discussed here are flow in bends, and the backwater length upstream from a control point.

Flow resistance

The balance between gravity and friction determines the mean velocity of a river, as can be seen by considering the force balance per unit bed area in a reach with macroscopically uniform flow (i.e. no overall acceleration or deceleration):

$$\tau = \rho g R S = \rho v^2 f/8 = \rho v^2/{C_f}^2 \quad (1)$$

Here τ denotes the mean bed shear stress (the gravity side of the balance) and ρ, g, R, v, and S denote water density, gravity acceleration, hydraulic radius (approximately equal to mean depth d except in very narrow channels), mean velocity, and channel slope (tangent of angle, negligibly different from sine of angle even in steep torrents). Bed shear stress varies considerably both between reaches and as discharge varies within a reach, with an overall range from ~1 to ~1000 N m^{-2}. The friction side of the balance (i.e. the resistance to flow) is parameterized in Equation (1) either directly by the non-dimensional Darcy–Weisbach friction factor f, which has the character of a drag coefficient, or inversely by the non-dimensional Chézy coefficient $C_f = (8/f)^{1/2} = v/(gdS)^{1/2}$. These, along with dimensional resistance indices such as Chézy's C, Manning's n, and the log-law roughness height, are expected to depend on channel characteristics such as bed grain size.

There is a large and continually growing literature on ways to predict flow resistance (see Ferguson, 2013 and Powell, 2015 for reviews), but almost all morphodynamic models that are intended to have wide applicability to alluvial rivers adopt one or other of two simple ways to specify C_f (or f). The first is to treat C_f as an unspecified constant (e.g. Tubino, 1991; Blom *et al.*, 2017a); the other is to represent the frictional resistance of a river bed by some roughness length scale k and assume C_f is a scale-invariant function of the relative submergence d/k. Very often the function is a 1/6 power law with k based on some bed grain diameter D (e.g. Parker, 1991; Griffiths, 2003; Parker *et al.*, 2007). This is equivalent to adopting the Manning equation, $v = d^{2/3}S^{1/2}/n$, with n proportional to $D^{1/6}$ as first suggested by Strickler (1923). The main alternative is the logarithmic relation $C_f = 2.5\ \log(11d/k)$ that is obtained by integrating the 'law of the wall' for turbulent boundary layers (Keulegan, 1938). Most models of bedrock river behaviour also assume either fixed C_f or fixed n, though in the latter case k should logically be an average of grain size and rock roughness weighted according to their relative extent (Johnson, 2014).

How well do these common scale-invariant assumptions hold over the full range of conditions? Figure 1A shows between-site variation in C_f at bankfull stage in 558 alluvial river reaches, using data drawn from Church and Rood (1983), Hey and Thorne (1986), Xu (2004), Kleinhans and van den Berg (2011), Bunte *et al.* (2013), Hassan *et al.* (2014), Trampush *et al.* (2014), and Li *et al.* (2015); see the online Supporting Information for details of sources and quality control. The median bed diameter D_{50} is used as k in this plot for reasons of data availability. There is considerable scatter in the plot, as expected since D_{50} is only a crude measure of bed roughness: it almost certainly underestimates resistance in coarse-bed rivers, and also in sand-bed rivers with bedforms. The 1/6 power line in this plot is Parker's (1991) version of Manning–Strickler with $n \propto (2D_{90})^{1/6}$, shown here on the assumption that $D_{90} = 2D_{50}$, which is a reasonable compromise between typical gravel-bed and sand-bed sorting. This relation plots above most of the data points, indicating that measured bankfull values of n are generally higher than is predicted from bed grain size. This is as expected, given the prevalence of dunes in sand-bed rivers and macro-roughness in shallower coarse-bed rivers. A fixed value of $C_f \approx 10$ might be adequate as a first approximation in broad-brush models with other major uncertainties. However, the median C_f value for sand-bed rivers in this data set is higher than the one for gravel-bed rivers (16 compared to 7) and the trend is more like a 1/6 power law, though with higher implied n values than in Parker's relation. A tendency for large rivers to have lower flow resistance helps them maintain broadly similar mean flow velocities, despite their typically lower mean bed shear stress.

When measurements at different low to high discharges within a reach are considered, it becomes much clearer that C_f is not invariant. Figure 1B plots nearly 3000 individual measurements of flow resistance at low to high discharges in a variety of channels with gravel or boulder beds (data compiled by Rickenmann and Recking, 2011). D_{84} is used as the roughness length scale here on the grounds that most resistance to flow is associated with larger-than-average grains. Parker's 1/6 power Manning–Strickler relation (now with D_{90} approximated by D_{84}) fits the data well at $10 < d/D_{84} < 100$, but not in shallower flows where resistance increases rapidly as submergence decreases. Another way of saying this is that n values calculated from flow measurements in coarse-bed rivers usually decrease as discharge increases, as demonstrated by Ferguson (2010).

The logarithmic resistance relation systematically underestimates resistance when D_{84} is used as the roughness height, but fits the trend of the data well if k is equated with a multiple of D_{84}; the version shown is that of Hey (1979) with $k = 3.5D_{84}$. Rickenmann and Recking (2011) found that the best-fitting predictor of all the equations they compared was the variable-power equation (VPE) of Ferguson (2007). The VPE is a smooth function joining asymptotes $C_f \propto (d/D_{84})^{1/6}$ in deep flows and $C_f \propto d/D_{84}$ in very shallow flows in which the larger clasts protrude close to or above the water surface. The deep-flow limit is effectively Manning–Strickler again, and the shallow-flow limit is one that is suggested by much experimental and theoretical research on roughness layers (e.g. Rickenmann, 1991; Gimenez-Curto and Corniero Lera, 1996; Lawrence, 1997; Nikora *et al.*, 2001; Aberle and Smart, 2003). One implication of this distinctive flow-resistance behaviour in small coarse-bed channels is that depth increases more slowly with discharge at a site, and velocity more rapidly, than is normally the case. This may also be true of bedrock rivers, since Ferguson *et al.* (2017) found a similar pattern to Figure 1B in four reaches of a small bedrock channel.

In both sand-bed rivers and shallow coarse-bed streams there is a factor-of-10 range in C_f at any given submergence ratio, which corresponds to a factor-of-5 range in predicted depth if discharge is known. As already noted, this uncertainty is the inevitable consequence of predicting resistance from grain size alone without consideration of bed form or structure. But the scatter does not prevent three conclusions being drawn about the trends in the data: (1) flow resistance can only be assumed invariant (fixed C_f) as a crude approximation; (2) it cannot be described by a simple power law over the full range of relative submergence; and (3) shallow flows, which are typically found in steep channels with coarse beds, have exceptionally high flow resistance and a different scaling on relative submergence than is appropriate for rivers with fine beds.

Flow in bends

Flow resistance determines the reach-average mean velocity of a river. Another aspect of river flow that is relevant to channel morphology is the helicoidal flow that occurs in meandering channels. I am not aware of any comparative data on this, but

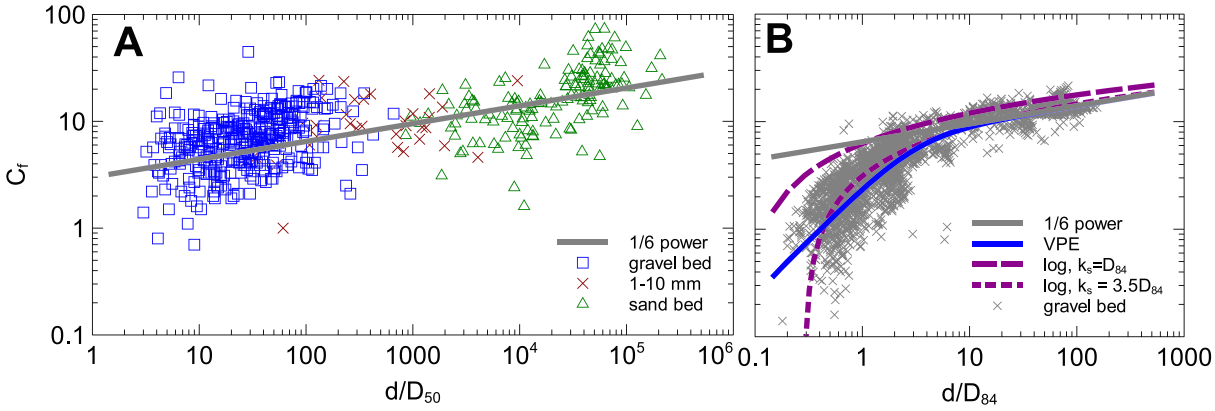

Figure 1. Flow resistance as a function of relative submergence in alluvial rivers. (A) Between-reach variation at bankfull discharge, with Parker's (1991) Manning–Strickler 1/6 power relation for comparison. (B) Within- and between-reach variation in gravel- and boulder-bed rivers, with three widely used resistance equations for comparison. Data in (A) are the author's compilation (see text and online Supporting Information). Data in (B) are those compiled by Rickenmann and Recking (2011) but filtered to exclude sites with D_{84} <10mm or significant woody debris. [Colour figure can be viewed at wileyonlinelibrary.com]

theory suggests that flow in bends is not scale invariant. Water flowing around a bend experiences a centrifugal force proportional to v^2/r, where r is the radius of curvature. This force is normal to the main flow so adds to the overall flow resistance, and in combination with a vertical velocity gradient it generates vorticity that is apparent as secondary circulation in the transverse-vertical plane. The ratio of head loss through this mechanism to total head loss along a reach scales with the square of the ratio d/r of flow depth to bend radius (Chang, 1988; Dingman, 2009) and can be considerable in laboratory experiments with r of order 1m (Leopold *et al.*, 1960; Ackers and Charlton, 1970). The angle δ by which near-bed flow deviates from the centreline direction in fully developed bend flow scales as $\tan \delta \propto d/r$ (Rozovskii, 1957; Engelund, 1974). For a given sinuosity, r is directly proportional to channel width (w) and meander wavelength (Leopold and Wolman, 1960) so scaling on d/r is equivalent to scaling on d/w. Empirical investigations of canal regime (e.g. Lacey, 1930) and downstream hydraulic geometry (e.g. Leopold and Maddock, 1953) show that w increases more rapidly than d with river discharge, so secondary circulation should become less pronounced in larger channels. Depending on the exact values of the w–Q and d–Q power-law exponents, an increase in discharge by a factor of 10^3 causes the deviation angle in a bend of given sinuosity to decrease by a factor of 2 to 3, centrifugal force per unit volume by a factor of 3 to 8, and relative energy loss by a factor of 5 to 10. These are fairly small departures from scale invariance, and evidently do not prevent large rivers like the Mississippi and some Amazon tributaries from meandering. They do, however, have implications for the pathways of bed load and suspended sediment in bends and might be a factor in differences in sedimentation style between main and side channels in large anabranched rivers.

Backwater length

Theoretical models of morphodynamics at reach scale generally assume uniform flow (sometimes called normal flow) in which velocity remains constant along the channel, there is no difference between mean bed slope, water surface slope, and energy slope, and the mean bed shear stress is proportional to the depth–slope product as in Equation (1). But flow is no longer uniform in reaches approaching a control point with lower or no surface slope: most obviously the coast, but also lakes, tributary junctions, and knickpoints. Instead, at a steady discharge the river's depth increases downstream, its velocity and water surface slope decrease downstream, and its bed shear stress is less than is suggested by the depth–slope product. However, during floods the water surface can be steeper than upstream (e.g. Phillips and Slattery, 2007). This backwater effect is perceptible to a distance $L = 0.7d/S$ upstream from the control point, where d and S are the depth and slope that would prevail in the absence of backwater (Samuels, 1989). It can be a long way in large lowland rivers with low gradients: for example, ~650km in the lower Mississippi (Nittrouer, 2013).

Backwater lengths for the worldwide selection of reaches in Figure 1A, estimated using local reach slope and depth, vary greatly because the data include rivers of all sizes. One way to remove the scale effect is to look at the ratio of L to channel width. This reveals a clear difference between sand-bed and gravel-bed rivers: median L/w is 115 in the former (interquartile range 45–246) but only 9 (4–21) in the latter. This contrast is because sand-bed rivers have much lower slopes than gravel-bed rivers of similar size. It means that backwater effects in gravel-bed rivers typically operate at the length scale of bars and bends, as is familiar from research on the maintenance of pool-riffle sequences, rather than extending up the channel network for distances comparable to the spacing of tributary junctions.

Limits to scale invariance: bed-material transport

The bed of an alluvial river may be static, partly mobile, or fully mobile depending on the grain sizes involved and the fluid force exerted on the bed. When transport occurs it may be largely or entirely by rolling and sliding (bed load), predominantly in suspension, or a mixture of these. Bed-material transport is an intrinsically stochastic process of particle entrainment, transport, and deposition driven by turbulent flow, but at the reach scale the interest is usually in the overall width- and time-averaged flux. Although it is possible to predict bed-material flux using stochastic models (Einstein, 1950; Ancey, 2020), scaling relations with bulk flow variables are usually preferred. Many different equations or sets of equations have been proposed. Some involve an invariance or a simple power law, but others involve departures from these. In this section I review some common assumptions and compare them with the data.

Entrainment threshold

It is commonly assumed that bed-material transport is insignificant until some threshold flow condition is exceeded. The threshold is sometimes defined as a critical value of discharge per unit width (Schoklitsch, 1934) or stream power per unit area (e.g. Bagnold, 1977) but is usually taken to be a critical value of the non-dimensional bed shear stress $\theta = \tau/(\rho_s - \rho)gD_{50} = dS/\Delta D_{50}$. Here ρ_s denotes sediment density, $\Delta = (\rho_s - \rho)/\rho$ is the submerged specific gravity of sediment, and θ (often called the Shields stress or Shields number) is the ratio of fluid drag to immersed grain weight. Shields (1936) showed experimentally that at high particle Reynolds numbers, which for quartz-density sediment in water means grain sizes exceeding 1 mm or so, beds of near-spherical particles of uniform size were fully mobilized at a more or less constant critical value $\theta_c \approx 0.06$. For sizes below 1 mm, θ_c decreases to a minimum for medium sand but then increases considerably for very fine sand and silt as the laminar sub-layer and intergranular cohesion become significant (Miller *et al.*, 1977). The value of θ_c for mixed-size coarse sediment varies by at least a factor of 2 according to how the threshold of motion is defined (nowadays usually as a critical value of a non-dimensional transport rate). It also depends on the extent of imbrication and other structuring of the bed, which varies over time as floods destroy bed structures and lower flows rebuild them (e.g. Reid *et al.*, 1985; Church *et al.*, 1998; Johnson, 2016). Buffington and Montgomery (1997) found that previously published estimates for individual gravel-bed rivers ranged from 0.030 to 0.086 and declined to suggest a 'best' value, but somewhere in the range 0.03–0.05 is generally accepted.

As will be discussed below, the assumption of an invariant critical Shields number is central to many methods for predicting bed-material flux and its consequences for morphological regime. But as just noted, θ_c varies over time in gravel-bed rivers and is systematically different for beds of very fine sand and silt. The invariance assumption also breaks down in two other circumstances: channels that are steeper than around 0.01 (1%), and beds that are bimodal mixtures of fine and coarse sediment.

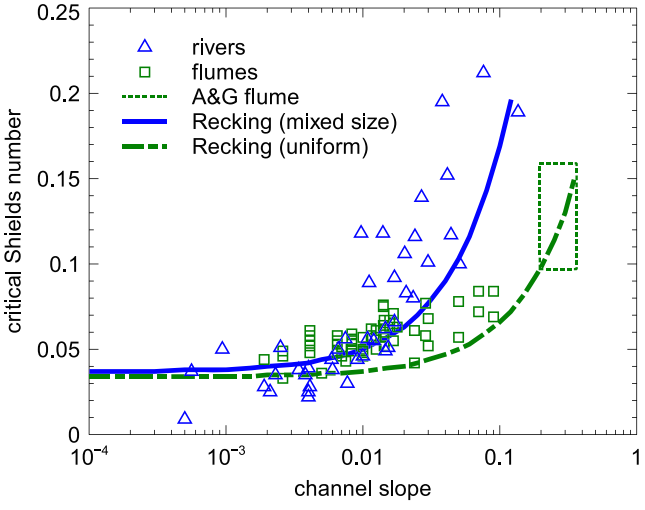

Figure 2. Variation of critical Shields number (θ_c) with channel slope. Field and flume data as in Ferguson (2012, his table 1), with the threshold of motion defined by a fixed non-dimensional sediment transport rate. Box labelled A&G is the envelope of a set of runs in an exceptionally steep flume (Armanini and Gregoretti, 2005). Curves are linear fits proposed by Recking (2009) for near-uniform sediment (flume experiments) and mixed-size sediment (coarse-bed rivers). [Colour figure can be viewed at wileyonlinelibrary.com]

Shields recognized that the downslope component of grain weight ought to reduce the entrainment threshold in very steep channels, until eventually the angle of repose is exceeded. However, this effect is negligible at angles below 20–30°. At more typical river gradients there is a perceptible empirical tendency in the opposite direction (Mueller *et al.*, 2005; Lamb *et al.*, 2008; Recking, 2009). An increase in θ_c with slope is apparent in flume experiments with well-sorted sediment as well as in field data, but at a given slope field estimates of the critical Shields number are higher (Figure 2). This presumably reflects the structuring of poorly sorted beds. Various linear (Mueller *et al.*, 2005; Recking, 2009) and power-law (Lamb *et al.*, 2008; Phillips and Jerolmack, 2019) relations between θ_c and S have been proposed. This tendency appears to be associated with high flow resistance in steep shallow streams (Recking, 2009; Ferguson, 2012) and can be predicted by force–balance calculations that allow for the non-logarithmic velocity profile in steep steams (Lamb *et al.*, 2008; Recking, 2009).

In beds with a bimodal size distribution the value of D_{50} falls somewhere between the two modal diameters, and θ_c calculated using D_{50} lies within the traditional range only if the bed consists dominantly of one or other fraction. For more equal proportions, θ_c is lower. For example, Wilcock *et al.* (2001) reported flume experiments with different proportions of poorly sorted gravel (median 13 mm) and well-sorted coarse sand (median 1 mm). As the sand content in the bulk mix increased from 15 to 34%, θ_c decreased from 0.035 to 0.014. The accepted explanation for this effect is that a small proportion of fine sediment can be hidden within a coarse framework, but higher proportions progressively fill the pore spaces until the bed is matrix-supported and sand is no longer sheltered by gravel. The mobility of coarse sediment increases to some extent, and that of sand to a greater extent.

Suspension threshold

At shear stresses just above the threshold for entrainment, grains move only by rolling or sliding along the bed. At higher stresses they start to saltate and may eventually be in permanent suspension, with their weight offset by upward impulses in the turbulent flow. The equivalence of mean bed shear stress (as given by the depth–slope product) with near-bed Reynolds stress implies that vertical velocity components scale with the shear velocity $u^* = (\tau/\rho)^{1/2}$, so the suspension threshold should be some fixed value of the ratio of u^* to the sediment settling velocity w_s. Bagnold (1966) proposed $u^*/w_s = 1$ as the threshold, and subsequent flume and river measurements broadly confirm this: suspension of medium or coarse sand is initiated at $u^*/w_s \approx 0.4$ (e.g. van Rijn, 1984) and transport is entirely in suspension by $u^*/w_s \approx 3$ (e.g. Ma *et al.*, 2020). However, the entrainment of fine sand or silt into suspension requires a higher shear velocity than these ratios suggest (van Rijn, 1984; Nino *et al.*, 2003), probably because such small grains are partly within the laminar sub-layer.

These suspension thresholds, together with Shields' entrainment threshold, can be used to delimit transport domains in a plot of τ against grain diameter D. To do this we need to know how w_s relates to D, and here we encounter a departure from simple power-law scaling as a result of the changing importance of different forces (Figure 3A). Grains smaller than ~0.1 mm experience a very small gravity force, settle slowly, and are retarded predominantly by viscous drag on their surfaces; this gives $w_s \propto D^2$ (Stokes' law). Grains larger than ~1 mm are subject to a much higher gravity force, settle rapidly, and are retarded predominantly by turbulence generation in their wake.

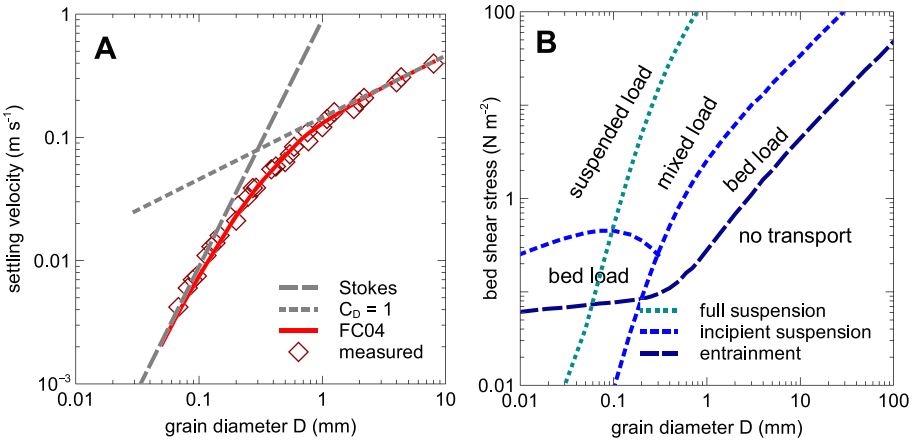

Figure 3. (A) Settling velocity of isolated quartz-density sediment grains in water at 20 °C, showing change in scaling with grain diameter D. Data points are laboratory measurements of Ferguson and Church (2004) and those collated by Hallermeier (1981). Curve labelled FC04 is the variable-power equation of Ferguson and Church (2004). (B) Transport mode of fluvial sediment as a function of grain diameter and bed shear stress. The entrainment threshold shown is that of Parker *et al.* (2003), with θ_c =0.030 for coarse grains. The full-suspension threshold is calculated using FC04 with u^*/w_s =3 and the incipient-suspension threshold uses u^*/w_s =0.4, with or without the fine-grain correction proposed by Nino *et al.* (2003, their equation 20). [Colour figure can be viewed at wileyonlinelibrary.com]

For any fixed value of the grain drag coefficient C_D, which depends mainly on grain shape, this implies $w_s \propto D^{1/2}$. The crossover between the power-2 and power-1/2 asymptotes has been fitted by a variety of equations, the simplest of which is one proposed and validated by Ferguson and Church (2004).

The nonlinearity in Figure 3A leads to nonlinearities in the boundaries between transport domains in Figure 3B. For grains larger than about 2 mm the entrainment and incipient-suspension thresholds are parallel straight lines (Shields: $\tau \propto D$, suspension: $u^* \propto D^{1/2}$), so a bedload domain exists for all coarse-bed rivers. There are, however, two complications: the critical stress to entrain size D depends also on the bed-average size D_{50}, with finer-than-average grains relatively harder to entrain than shown in Figure 3B because they are sheltered by larger ones; and the high grain diameters towards the right-hand end of Figure 3B are typically found in steep channels, where the threshold Shields number for entrainment is higher than shown, making the bedload transport domain narrower (Ferguson, 2012; Phillips and Jerolmack, 2019). Incipient suspension requires a shear stress almost an order of magnitude higher than for incipient bed load ($\theta \approx 0.21$ instead of 0.03), and full suspension would require the Shields number to be far higher still ($\theta \approx 12$), which never occurs in gravel-bed rivers.

As grain size declines below 1 mm the scaling changes. The entrainment threshold curve becomes flatter because grain cohesion and the laminar sub-layer start to become significant, and the suspension thresholds become steeper because of the switch towards Stokes settling. This might seem to imply that there is no bed load domain for grains finer than about 0.2 mm (where the bed-entrainment and incipient-suspension curves cross in Figure 3B), but the experimental results of Nino *et al.* (2003) suggest that fine beds cannot be entrained directly into suspension: instead, a bedload domain does continue to exist over a narrow range of very low shear stresses (around 0.1–0.2 N m^{-2}). This implies that any fine sediment that settles from suspension has a tendency to remain on the bed.

Bankfull Shields number

Most sediment is transported in flood conditions, so it is of interest to ask whereabouts in the transport-domain diagram rivers plot when flowing at their bankfull discharge. Opinion in the literature is divided. There is a widespread view (e.g. Howard, 1980; Hey *et al.*, 1982; Dade and Friend, 1998; Church, 2006; Dunne and Jerolmack, 2018) that most rivers fall into two distinct groups: gravel-bed rivers (GBRs) with bankfull shear stress only slightly above threshold and transport entirely as bedload, and sand-bed rivers (SBRs) with bankfull shear stress far above threshold and transport mainly or entirely in suspension. In this view, the bankfull Shields number in GBRs is typically <0.1, whereas that for SBRs is typically ≥1. But some researchers have argued that there is a continuum, with bankfull Shields number varying continuously with D_{50} in a predictable way (Wilkerson and Parker, 2011; Trampush *et al.*, 2014; Li *et al.*, 2015). For example, Trampush *et al.* (2014) fitted a non-dimensional relation equivalent to $\theta_{bf} \propto D_{50}^{-0.77}$.

Estimated Shields numbers at bankfull discharge are plotted against bed D_{50} in Figure 4A using the same worldwide data set as in Figure 1A. Transport domains are distinguished using the same thresholds as in Figure 3B, though now plotted as critical values of θ instead of τ. That diagram was for the grain size in transport, not the average size in the bed, but these are essentially the same in most sand-bed rivers so the low-D parts of the threshold curves are directly transferable. Gravel-bed rivers generally have much less well-sorted beds. The critical Shields number for entrainment of size D_i in a bed of median size D_{50} varies almost inversely with D_i/D_{50} because of hiding and protrusion effects (e.g. Ashworth and Ferguson, 1989; Parker, 1990), so the right-hand end of the entrainment curve in Figure 4A should really be a band within which transport is partial and size-selective. Likewise, the horizontal parts of the suspension threshold curves should be slightly lower since grains in suspension are likely to be from the fine tail of the bed size distribution.

Figure 4A lends some support to both schools of thought in the literature. Two features are superficially consistent with the continuum view: there is a continuous spread of values of the bankfull Shields number, with lower values in some SBRs than in some GBRs; and if the data points for all grain sizes are viewed collectively, a general power-law trend with an exponent of about −1/2 can be discerned. However, an overall inverse trend is inevitable because D_{50} is in the denominator of θ_{bf}, and the data points clearly form separate fine-bed and coarse-bed groups with a relative shortage of 1–10 mm beds (only 33 reaches out of 558). Reaches in the fine group plot

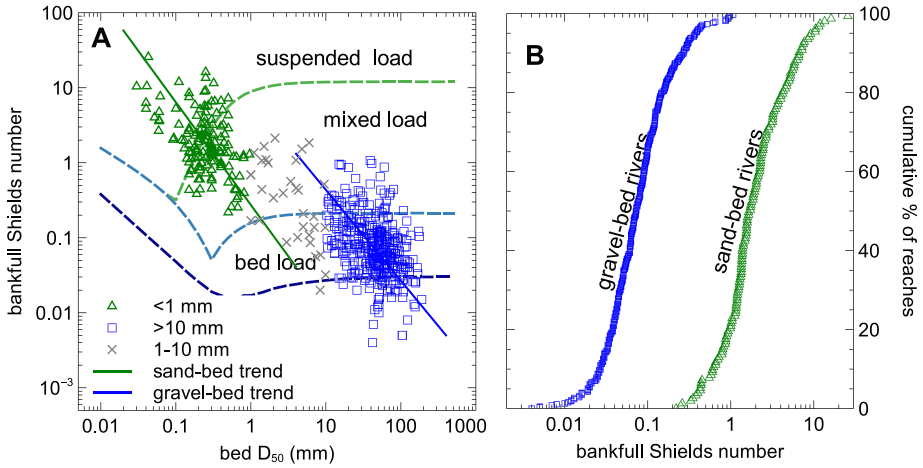

Figure 4. (A) Relation between Shields number at bankfull discharge (θ_{bf}) and median bed grain size in 558 alluvial reaches (same data as Figure 1A), overlaid on thresholds for entrainment, incipient suspension, and full suspension. Displayed trendlines for gravel-bed (D_{50} >10mm) and sand-bed (D_{50} <1mm) reaches are principal-axis fits. (B) The very different frequency distributions of θ_{bf} for gravel- and sand-bed reaches. [Colour figure can be viewed at wileyonlinelibrary.com]

entirely within the mixed- and suspended-load domains, whereas reaches with coarse beds mostly plot within the bed load domain. An inverse relation between θ_{bf} and D_{50} is apparent within each group. The trendlines shown were fitted by the principal-axis method, which allows for similar amounts of measurement error in both variables (see online Supporting Information for a discussion of sources of measurement error and regression methods to allow for it). They are offset horizontally in the overlap zone at $\theta_{bf} \approx 0.5$. This offset is even clearer in Figure 4B, which shows that gravel-bed (D_{50} >10mm) and sand-bed (D_{50} <1mm) reaches both have lognormal distributions of θ_{bf} with a similar spread, but the means differ by a factor of about 30. The groups therefore correspond to far-from-threshold SBRs and near-threshold GBRs.

Approximately two-thirds of the sand-bed reaches in Figure 4A plot within the mixed-load domain and one-third in the fully suspended domain. Grain size, rather than river size or slope, is the main factor here: reaches with $D_{50} \geq 0.5$mm experience mixed-load transport even at bankfull discharge, whereas almost all of those with $D_{50} \leq 0.2$mm have a fully suspended load in those conditions, though with some bed load at lower discharges. This difference reflects the switch from inertial to Stokes settling over this range of grain size. The few reaches with 1–10mm beds are equally divided between the bedload and mixed-load domains.

The great majority of gravel-bed reaches plot within the bedload regime but some are below the entrainment curve or above the incipient-suspension curve. It must be remembered that θ_{bf} here is calculated using mean depth, so it is possible for deeper parts of the channel to have a mobile bed despite a low overall Shields number. The highest gravel-bed Shields numbers are all from small steep reaches with gradients exceeding 5% and bankfull discharge mostly below 10 $m^3\ s^{-1}$. Since slope is in the numerator of θ a positive correlation between them is hardly surprising, and it has previously been noted by Mueller *et al.* (2005) and Phillips and Jerolmack (2019).

Bed-material flux

If significant entrainment of bed material begins at some non-zero critical value of a flow variable such as bed shear stress, the transport rate ought to be a function of the excess of that variable over its critical value. Most of the many equations proposed for bed-material flux in gravel-bed rivers are of this form. Well-known examples are $\Phi \propto (\theta - \theta_c)^{3/2}$ or $q_s \propto (\tau - \tau_c)^{3/2}$ (Meyer-Peter and Müller, 1948), $q_s \propto (\omega - \omega_c)^{3/2}$ (Bagnold, 1977), and $\Phi \propto (\theta - \theta_c)^{4.5}/\theta^3$ (Parker, 1979). In these equations, $\omega = \rho g q S = \tau v$ is stream power per unit bed area, q_s is the volumetric transport rate per unit width, and $\Phi = q_s/(\Delta g D_{50}^3)^{1/2}$ is a non-dimensional form of q_s that was introduced by Einstein (1950). Each of these equations is asymptotically a 3/2 power relation, but only at shear stresses far higher than are ever reached in gravel-bed rivers. In near-threshold conditions the rate of change of flux with stress is very high, in accordance with observational evidence of a rapid increase in the number and size of grains entrained (Wathen *et al.*, 1995; Wilcock and McArdell, 1997).

In regime theories and one-dimensional numerical models, the shear stress or stream power that is used to predict sediment transport is a width-averaged or reach-averaged value. If there is spatial variation around the average, and flow is not far above threshold (as in most gravel-bed rivers), the nonlinearity of the relation between local shear stress and local transport rate means that the average stress underestimates the overall transport rate (e.g. Ferguson, 2003). This and several other problems associated with the use of the depth–slope product estimate of shear stress are discussed by Yager *et al.* (2018).

In sand-bed rivers the critical shear stress is negligibly low (~0.1 $N\,m^{-2}$; see Figure 3B), allowing a simple power law to be used to predict sediment flux. However, measurements suggest the exponent is higher than 3/2. The best-known equation for sand flux is that of Engelund and Hansen (1967), which can be written as $\Phi \propto \theta^{5/2}$ with a prefactor that depends on C_f. The entrainment threshold is sometimes also omitted when predicting bedload transport in gravel-bed rivers. Some river engineers in the Netherlands follow Struiksma (1985) in using a power-law relation between q_s and v for all rivers, but with a higher exponent for GBRs than SBRs; for example, Crosato and Mosselman (2009) used 4 for SBRs but 10 for GBRs. Barry *et al.* (2004) proposed a simple Q_s–Q power law for GBRs and found that it worked well after the exponent and prefactor were calibrated using catchment characteristics. A hybrid equation proposed by Recking (2013) links a 5/2 power high-θ asymptote with a 6.5 power low-θ asymptote and takes account of the effects of slope and bed sorting on θ_c. It outperformed several better-known equations in a test by Hinton *et al.* (2018).

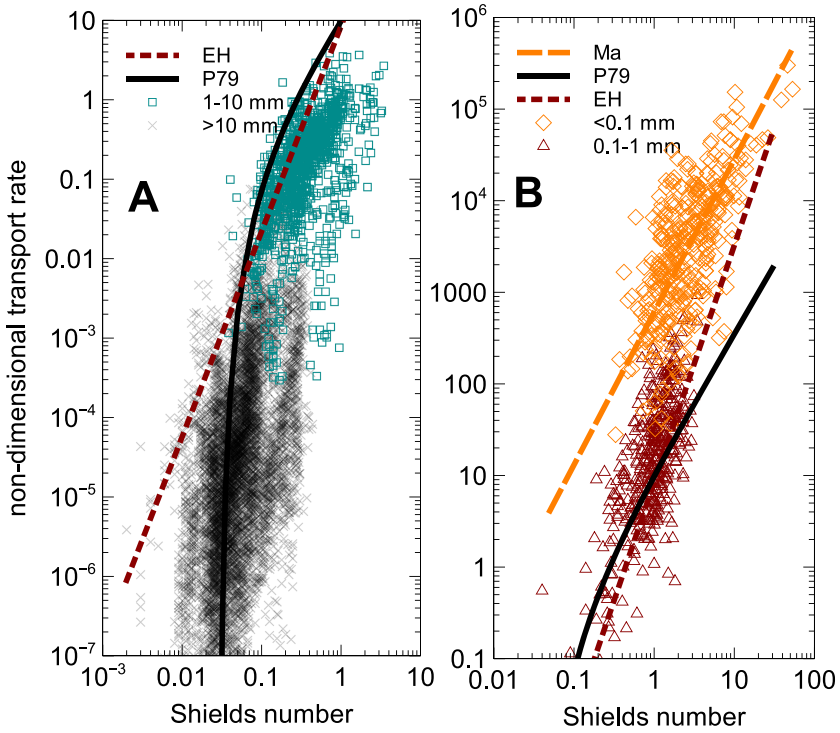

Figure 5. Field measurements of bed-material transport in rivers with different ranges of bed D_{50}. Coarse-bed data in (A) are from Recking *et al.* (2016) with sand-bed reaches excluded; fine-bed data in (B) are from Ma *et al.* (2020). Curves labelled P79, EH, and Ma are equations proposed by Parker (1979) for gravel, Engelund and Hansen (1967) for sand, and Ma *et al.* (2020) for silt. [Colour figure can be viewed at wileyonlinelibrary.com]

What do measurements of bed-material transport in rivers show? Figure 5 shows Φ–θ plots based on measurements at many discharges within each of a wide variety of reaches, using the largest data compilations I can find. To help isolate any differences according to grain size, rivers with coarse beds (data of Recking *et al.*, 2016; 8630 measurements) are plotted separately from rivers and unlined canals with fine beds (data of Ma *et al.*, 2020; 783 measurements) and two ranges of bed D_{50} are distinguished within each plot. The reaches in which measurements were made are very diverse, with slopes from 2.1×10^{-6} to 0.045, bed D_{50} from 0.02 to 83 mm, and discharge from <1 to >26000 $m^3\ s^{-1}$.

The measured bedload fluxes range even more widely, with a three orders-of-magnitude range within the fine gravel, coarse sand, and fine sand subsets of the data and an even greater range for coarse gravel beds. When converted back to the approximate number of grains passing the measurement point, the lower end of Figure 5A corresponds to a few small pebbles per metre width per second and the upper end to thousands of granules. The lower part of Figure 5B corresponds to millions of fine sand grains and the upper part to billions of silt grains, again per metre per second. Transport efficiency in the sense of work done per unit stream power (Bagnold, 1966) is proportional to $q_s/\tau v$ and therefore increases diagonally upwards and leftwards for any given grain size.

The coarse-bed measurements in Figure 5A do not follow a simple power law over the full range of conditions. The >10 mm data could reasonably be described by a power law with an exponent of about 6, but the 1–10 mm data are roughly parallel to the 5/2 power Engelund–Hansen sand-bed equation. Transport in most of the 1–10 mm reaches is purely bedload at lower discharges according to the thresholds plotted in Figure 4, but enters the mixed-load domain at higher discharges. The excess-stress equation of Parker (1979) fits the >10 mm data reasonably well, but overestimates transport rates over finer beds. The equation proposed by Recking (2013) cannot be plotted as a single curve because the predicted flux depends on slope and D_{84}/D_{50} ratio, which vary between reaches, but for typical values of these additional variables it predicts lower fluxes than Parker's relation.

There is a wide scatter around the trends in each part of Figure 5, particularly for reaches with coarse (>10 mm) beds. In this subset of the data (Figure 5A), measured transport rates at a given Shields number range over four orders of magnitude and a given transport rate can be generated by a wide range of Shields numbers. Significant transport in coarse-bed reaches at mean Shields numbers below the traditional threshold for entrainment can be explained by within-reach spatial variation: even if most of the bed is immobile, entrainment can occur where shear stress is locally higher than average (e.g. thalwegs) or critical stress is lower than average (e.g. sand-rich patches within the reach or immediately upstream). Negligible transport at Shields numbers around 0.1, well above the traditional threshold, can be explained in several ways. Form drag due to macroroughness reduces the effective shear stress available for bedload transport (e.g. Yager *et al.*, 2007; Nitsche *et al.*, 2011; Ferguson, 2012), θ_c may be unusually high because of bed structures, and potentially mobile finer grains may be sheltered by protruding coarse grains (Recking, 2013; MacKenzie *et al.*, 2018). Recking (2010, 2013) proposed that θ_c for poorly sorted beds should be calculated using D_{84} as well as D_{50}, and that Φ and θ should be scaled using D_{84} not D_{50}. This makes no difference to the scatter in plots like Figure 5A, but reduces flux predictions for more poorly sorted beds.

Measured transport rates in sand-bed rivers (Figure 5B) plot systematically above the excess-stress equation of Parker (1979), more so the finer the bed material. The Engelund–Hansen equation (and thus also Recking's, 2013 hybrid equation) fits the 0.1–1 mm data well, but reaches with D_{50} <0.1 mm have higher fluxes at a given Shields stress and a slightly flatter trend in the plot. This may reflect differences in transport mode. Comparison of the transport-rate data with

the shear stress thresholds in Figure 4 suggests that reaches with D_{50} >0.4 mm have a mixed bed/suspended load at all discharges, and those with D_{50} in the range 0.1–0.4 mm also have a mixed load at most discharges though with full suspension at high discharges. In contrast, most of the measurements with D_{50} <0.1 mm are in the full-suspension domain, with mixed load only at the lowest discharges. Almost all of these measurements are from the Yellow River in China, and Ma *et al*. (2020) proposed a new 5/3 power relation for them, as shown in Figure 5B. Transport efficiency varies greatly within each grain-size subset of the data, but the scaling of Φ by $D_{50}^{3/2}$ implies that efficiency is generally higher in reaches with finer beds.

The message of this analysis is that the relation between shear stress and bed-material flux can be approximated by a simple power law only over a limited range of D_{50}, with a different exponent depending on the range concerned: very high for coarse beds, but progressively lower for finer beds. No single threshold-excess relation holds over the full range, and excess-stress predictions for coarse beds are extremely sensitive to the assumed value of the threshold stress.

Scale relations for bankfull channel dimensions

There is a long history of attempts to predict the width and depth of alluvial channels that, averaged over a period of years, are just able to convey the water and sediment supplied from upstream. The pioneering 'regime theory' of canal engineers (e.g. Lacey, 1930) and 'downstream hydraulic geometry' of Leopold and Maddock (1953) was empirical, but has subsequently been complemented by theoretical and hybrid approaches involving assumptions about flow and transport processes, optimality, and bank strength (e.g. Henderson, 1961; Parker, 1979; Eaton *et al*., 2004; Millar, 2005). The standard scaling variable is river discharge, since the hydrological regime is what provides the driving force for sediment transport, and the integrated effect of different discharges is almost always represented by a single 'channel-forming' or 'dominant' discharge. Leopold and Maddock used mean discharge for reasons of data availability. Most previous and subsequent work has preferred bankfull discharge (Q_{bf} hereafter) on the grounds that transport capacity is highest at that stage, but mean or median annual flood is sometimes used (e.g. Bray, 1982).

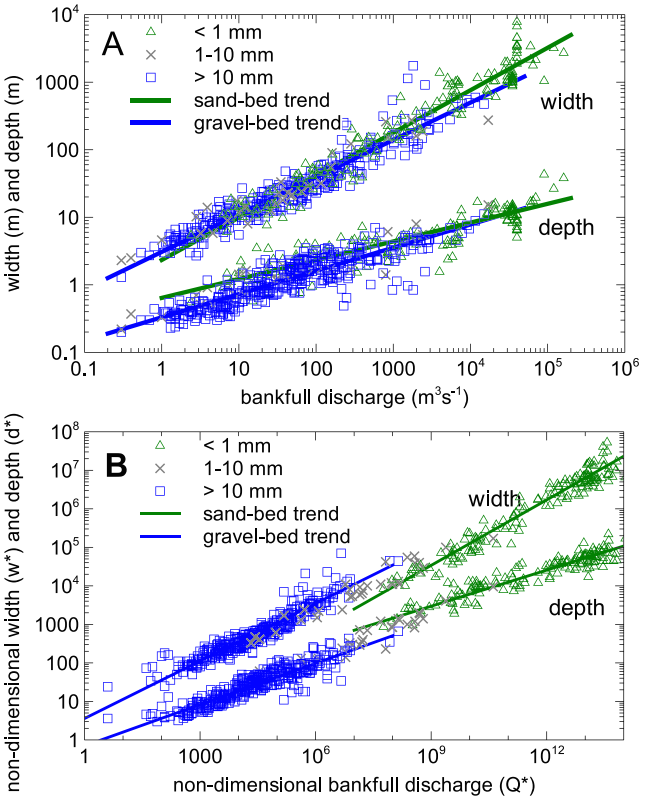

Figure 6. (A) Bankfull width and mean depth in 558 alluvial reaches (data as in Figure 1A) as functions of bankfull discharge. (B) Non-dimensional plot of the same data with each variable scaled using bed D_{50} grain size. Trendlines are separate principal-axis fits for reaches with D_{50} >10 mm and D_{50} <1 mm. [Colour figure can be viewed at wileyonlinelibrary.com]

The simplest possible scaling for channel dimensions is that rivers of all sizes have the same cross-section shape. If they also have the same Froude number, as when designing flume experiments that are intended to be scale models of rivers (e.g. Ashmore, 1991), bankfull channel width (w_{bf}) and mean depth (d_{bf}) must both vary as $Q_{bf}^{2/5}$ (e.g. Griffiths, 2003). But in reality, rivers at bankfull have a wide range of Froude numbers (from <0.1 to ~1 in the present data set), and the geometric scaling is allometric: width increases more rapidly with discharge than depth does. Regime theory for canals (Lacey, 1930; Simons and Albertson, 1960) and rivers (Blench, 1969) proposed that $w_{bf} \propto Q_{bf}^{1/2}$ and $d_{bf} \propto Q_{bf}^{1/3}$, with prefactors that depend on grain diameter. Leopold and Maddock (1953) used regression analysis to fit power laws and found exponents of 0.50 for width and 0.40 for depth. These simple scalings are not dimensionally balanced, so from Parker (1979) and Bray (1982) onwards some researchers have fitted power-law relations between variables made non-dimensional using median bed grain diameter: $w^* = w_{bf}/D_{50}$, $d^* = d_{bf}/D_{50}$, and $Q^* = Q_{bf}/(\Delta g D_{50}^5)^{1/2}$. Others have used log–log multiple regression to relate width or depth to discharge along with slope and/or grain size (e.g. Lee and Julien, 2006).

In this section I examine how universal the width-discharge and depth-discharge scalings are, using the same data compilation as for bankfull flow resistance (Figure 1A) and transport mode (Figure 4) and distinguishing reaches with coarse, intermediate, and fine beds.

Both width and depth follow linear trends over a 10^6-fold range of discharge in the log–log plot (Figure 6A), and width increases more rapidly than depth so that w/d tends to increase. This is as expected from previous work, but there are two differences from the traditional universal scaling: a small but systematic difference between gravel- and sand-bed rivers, and a more rapid increase in width with discharge than the traditional 0.5 power relation. Separate principal-axis fits (to allow for measurement error in Q_{bf}) are shown in Figure 6A for gravel-bed and sand-bed reaches, defined for this purpose by D_{50} >10 and <1 mm, respectively. They indicate that width increases slightly faster with discharge in SBRs than GBRs (exponent 0.63 compared to 0.55), and depth does the opposite (0.28 compared to 0.35). At low discharges SBRs tend to be narrower than GBRs, and at high discharges SBRs tend to be wider than GBRs. The differences in the exponents are not large but they appear to be systematic judging by the lower and upper limits that are provided by the OLS and reverse-OLS estimates of the exponents. For the width–discharge relation these are 0.62–0.66 for sand-bed reaches compared to 0.54–0.60 for gravel-bed reaches; for the depth–discharge relation, they are 0.27–0.33 (sand) compared to 0.34–0.44 (gravel). The width exponent is clearly greater than 0.5 for both types of reach, whereas the depth exponents are compatible with the traditional values of 1/3 or 0.4.

These downstream hydraulic geometry relations are visually much better defined than the flow-resistance and transport-rate relations in Figures 1 and 5, but there is still a

factor-of-2 scatter around the width and depth trends. The points farthest from the fitted trendlines are braided GBRs in New Zealand and braided or anabranched sand/silt-bed reaches in China, with unusually high width and low mean depth in both cases. Omitting these multi-thread reaches makes no difference to the SBR exponents and minimal difference to the GBR exponents.

Differences between gravel-bed and sand-bed hydraulic geometry are also apparent in the non-dimensional version of the plot (Figure 6B). The sand-bed w^*–Q^* relation is steeper (exponent 0.57, compared to 0.50 for gravel-bed reaches) and is lower by a factor of 3 at $Q^* \approx 10^7$–10^8 where large GBRs and small SBRs overlap. Conversely, the sand-bed d^*–Q^* relation is flatter (exponent 0.31, compared to 0.36 for gravel-bed reaches) and is offset upwards in the overlap zone. These results are qualitatively similar to what Parker *et al.* (2007) and Wilkerson and Parker (2011) found for GBRs and SBRs, respectively, by regression analysis of smaller data sets using different non-dimensional variables. The offsets show that for a given value of Q^*, gravel-bed reaches have a considerably higher width–depth ratio than sand-bed reaches. That is not surprising: Q^* is scaled by $D_{50}^{2.5}$ and D_{50} is of order 10^2 higher for gravel than sand, so gravel-bed Q is several orders of magnitude higher than sand-bed Q at the same value of Q^*. It may be concluded that the way D_{50} is used to make w^*, d^*, and Q^* non-dimensional creates more problems than it solves and does not adequately capture the effects of sediment characteristics on bankfull morphology. Unconstrained log–log multiple regression using the full Figure 6 data set does no better. The OLS regression of width on discharge already has a high R^2 value (0.94) and using D_{50} and slope as additional predictors improves this by only 0.002. Using all three predictors for depth makes slightly more difference, with R^2 increasing from 0.84 to 0.88, but the improvement in fit remains small.

Differences in bank, rather than bed, characteristics are an obvious candidate for explaining some of the remaining variance in width and depth. Information on bank characteristics is not available in the data sources used to construct Figures 4 and 6, but it is often inferred that the higher the bankfull Shields number relative to the threshold based on D_{50}, the stronger the banks must be (e.g. Millar, 2005; Parker *et al.*, 2007). Channels bounded entirely by homogeneous non-cohesive sediment will become wider and shallower until their banks are at the threshold of motion; the transverse distribution of shear stress then means that the central part of the bed will be somewhat above threshold, with θ_{bf}/θ_c not far above 1 (Parker, 1978). But many river banks are strengthened by cohesive sediment deposited from suspension and by plant or tree roots. There is empirical evidence that bankfull width for a given discharge varies with the density of vegetation cover (Andrews, 1984; Hey and Thorne, 1986), and wide shallow laboratory channels become narrower if plant seeds are added so that marginal sediment becomes stabilized by vegetation (e.g. Gran and Paola, 2001). As Kleinhans (2010) explained in a detailed review of the balance between bank erosion and floodplain construction, there is a positive feedback with vegetation both reducing near-bank flow velocity and increasing bank strength. However, a scale effect exists: the protective effect of vegetation on cut banks becomes less and less effective as banks become higher relative to plant rooting depth, allowing undercutting to occur. Eaton and Millar (2004) and Eaton and Church (2007) compared observed downstream hydraulic geometry with the predictions of a regime model that represents bank strength by a friction angle and concluded that bank strength must on average decrease with increasing river discharge.

Discussion

The three preceding sections of this paper give a clear answer to one of the initial questions: departures from simple scaling exist in all aspects of river morphodynamics. After summarizing what these departures are, I consider in turn the main candidates for 'distinctive' channel types and whether they are associated with discontinuities in simple scaling.

Departures from simple scaling

Channel dimensions come nearest to universal scaling, with simple power laws giving a good visual fit to downstream hydraulic geometry over a 10^6 range of bankfull discharge. But closer analysis shows that the trends for gravel-bed and sand-bed rivers are not identical and do not come together when each variable is scaled by grain size (Figure 6), and there is considerable scatter about each relation.

The section on river flow identified several departures from simple scaling. Flow resistance as quantified by C_f can only be assumed invariant in very broad-brush models, and nor does it follow a simple power law over the full range of the submergence ratio d/D: the exponent varies from 1/6 or less in deep flows to 1 or more in very shallow flows (Figure 1B). A 1/6 power relation is a reasonable approximation for intermediate and deep flows, but its best fit to measurements implies considerably more resistance than in the traditional Manning–Strickler relation. The biggest departures from 1/6 power scaling are for shallow flows in relatively small, usually steep, channels with coarse beds. This is associated with form drag on individual large clasts, spill losses, and a non-logarithmic velocity profile. At the other extreme, very large rivers are distinctive in two other flow attributes: they have appreciably weaker secondary circulation in bends, and backwater affects them over far greater distances than in smaller and steeper channels.

The discussion of bed-material transport identified departures from simple scaling in all aspects of the process. The commonly made assumption that significant transport commences at a fixed value of the Shields number breaks down in steep channels, where the threshold is higher (Figure 2), and also for bimodal beds and very fine beds. Grain-settling velocity varies with the square root of diameter for coarse sand and granules but with diameter squared for silt, as the balance between inertial and viscous forces changes. This enables fine-bed material to be transported in suspension rather than as bed load (Figure 3), and is the physical basis for distinguishing coarse-bed from fine-bed rivers. Bed-material flux varies most sensitively with shear stress in reaches with gravel beds, and least so for reaches with beds of silt and fine sand (Figure 5). This ties in with the poorly sorted nature of coarse stream beds and the relatively low Shields stresses exerted on them, which in combination lead to strongly size-selective bedload transport at a highly variable rate over a largely immobile bed.

Distinct channel types?

The calculated bankfull Shields numbers for the 558 alluvial reaches plotted in Figure 4, and the transport modes inferred from them, support the distinction between coarse-bed and fine-bed rivers that has been made by several previous authors (e.g. Howard, 1980; Dade and Friend, 1998; Church, 2006; Dunne and Jerolmack, 2018). Two main groups are apparent in the data: coarse-bed reaches with bankfull Shields numbers relatively close to threshold and thus a bedload transport regime, and fine-bed reaches with high Shields numbers and

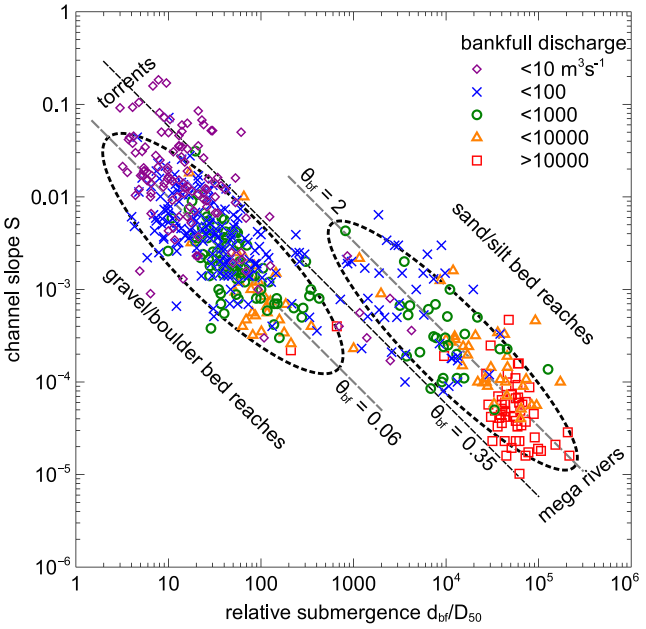

Figure 7. Channel slope and relative submergence at bankfull discharge in 558 reaches (data as in Figure 1A), showing separation between coarse-bed reaches (Shields number θ_{bf} close to threshold) and fine-bed reaches (θ_{bf} far above threshold). Colour coding by discharge highlights distinctive end-member types: small steep coarse-bed torrents and very large low-gradient ('mega') sand-bed rivers. [Colour figure can be viewed at wileyonlinelibrary.com]

a dominantly suspended load regime. The concentration into two distinct groups is equally clear when θ_{bf} is disaggregated into its two components, slope and relative submergence (Figure 7). Diagonals in this plot are lines of constant bankfull Shields number. Three such lines are shown in the diagram: typical values θ_{bf} =0.06 and 2 for coarse- and fine-bed reaches, respectively, and θ_{bf} =0.35 as an approximate threshold between the two groups at moderate and low channel gradients.

Different ranges of bankfull discharge are indicated in Figure 7 by colour-coding the data points. The pattern within each group is that higher discharges tend to be associated with higher relative submergence and gentler slope. This is in accordance with the positive correlation between bankfull depth and discharge (Figure 6A) and the tendency for bigger rivers to have lower slopes. In this particular data compilation, all coarse-bed reaches have d/D_{50} <700 and all fine-bed reaches have d/D_{50} >700, but relatively shallower sand-bed reaches certainly exist. Relatively deeper coarse-bed reaches probably also exist, for example where the Tsangpo and Yangtze rivers first emerge from their gorges. The biggest rivers in terms of discharge all have fine beds and very low gradients. They are labelled 'mega rivers' in the diagram and are discussed later, as are the very steep and relatively high-θ 'torrents' at the opposite corner of the diagram.

The difference in transport regime between typical coarse- and fine-bed reaches is a consequence of the scaling discontinuity in settling velocity (Figure 3), but this does not by itself explain why few rivers seem to have a bed surface D_{50} in the 1–10mm range. Two possible explanations exist that do not involve scaling. The first is that rock weathering does not generate much 1–10mm sediment. This may be true for particular lithologies (e.g. Yatsu, 1957; Wolcott, 1988), but it seems implausible at global scale across all lithologies. A second possibility is that the present data compilation underestimates the prevalence of 1–10mm river beds. The compilation includes rivers of all sizes in a wide range of tectonic and climatic settings, but the data are geographically biased, with North America heavily over-represented and Africa and Australia particularly under-represented. The colour coding in Figure 7 suggests that small sand-bed streams may also be under-represented, and in arid environments they may have relatively low bankfull Shields numbers because their banks are not strengthened by mud or vegetation.

A third alternative is that the downstream fining of bed material that occurs in most river systems is somehow accelerated where the surface D_{50} drops below ~10mm. This recognizes that reaches exist within river networks, and ties in with the discussion earlier in the paper of departures from simple scaling of sediment entrainment. Downstream transitions from gravel to sand bed can be quite abrupt relative to the total length of the river system (Yatsu, 1957; Smith and Ferguson, 1995; Radoane *et al.*, 2008; Frings, 2011; Venditti and Church, 2014), though some are gradual (e.g. Singer, 2008). The transition involves an increase in the sand content of a predominantly gravel bed to the point that sand overflows the pore spaces and starts to smooth the surface, leading to the preferential increase in sand mobility that was discussed above. Extra sand may be supplied from the drainage basin via sand-bed tributaries (Smith and Ferguson, 1995; Radoane *et al.*, 2008), or from upstream through the abrasion of gravel (Yatsu, 1957; Kodama, 1994). In situations where shear stress declines downstream, gravel becomes progressively less mobile and sand-rich bed load is deposited on the aggrading bed (Smith and Ferguson, 1995; Venditti and Church, 2014). Downstream fining of the surface means that the maximum grain size that can infiltrate into pore spaces declines (from 2to 0.05mm in the River Rhine; Frings *et al.*, 2008), so aggrading sand mostly remains on the surface, accelerating the downstream fining. Some sand will also settle from the wash load and can then only move as bed load, as noted with regard to Figure 3B and explained in detail by Lamb and Venditti (2016). Whatever the cause of the increase in sand content, the bulk and surface D_{50} values decrease and the river bed changes downstream to a general sand matrix with gravel patches on bar tops (Singer, 2008; Ferguson *et al.*, 2011; Venditti and Church, 2014), near the outer banks of bends (Frings, 2011), and in depressions between sandy bedforms (Ferguson *et al.*, 2011). The threshold shear stress is now much lower, so that transport is more efficient (see Figure 5) and streamwise continuity of bed-material flux can be maintained over a lower gradient (Howard, 1980; Blom *et al.*, 2017b).

Of the 59 reaches in the highest discharge class in Figure 7, only three have gravel or gravel/sand beds. The others all have sand beds, mostly towards the finer end of that size class (D_{50} 0.06–0.4mm, median 0.21mm), and 45 of them have bankfull discharges of at least 30000 $m^3 s^{-1}$ (over 100000 $m^3 s^{-1}$ in one reach of the Amazon). These very large fine-bed reaches correspond to what Latrubesse (2008) termed 'mega rivers'. Fine grain size together with great depth (d_{bf} typically 10–20m) means they have very high relative submergence. They also all have extremely low gradients (0.000016–0.00047, median 0.000043), and thus plot towards the bottom-right corner of Figure 7 as end-members of the sand-bed group of reaches. There is no sharp distinction between these reaches and those in smaller sand-bed rivers, but they are extreme cases in more respects than just size and gradient. Their bed material is sufficiently fine that transport is predominantly in suspension at high discharges as a consequence of the scaling change in settling velocity (Figures 3 and 4A). Sediment transport is therefore unaffected by lateral bed slopes and instead follows the water flow direction, promoting vertical bar accretion and conversion to floodplain (Nicholas, 2013). The difference between low-flow and flood-peak depth in such large rivers is considerable (7–12m at sites on the Amazon according to Mertes

et al., 1995), especially when compared to the very gradual longitudinal change in elevation (of order 1 m per 10 km along the river). This helps explain why extensive overbank flooding into side channels and seasonal floodplain lakes is common in mega rivers (Latrubesse, 2008; Ashworth and Lewin, 2012), with associated loss of suspended sediment from river to floodplain. Backwater lengths are very high (typically in the 100–1000 km range); this has been shown to affect flood-wave behaviour along the Amazon (Trigg *et al.*, 2009) and may be relevant in other large lowland rivers. The very high discharges of mega rivers imply high width/depth ratios (Figure 6A) and, at least in the case of a single-thread river, weaker helicoidal flow. This may be one of the reasons why few of Earth's largest rivers have meandering planforms (Latrubesse, 2008), though another factor is the incorporation of side channels into an anastomosing planform in which meandering is a property of each channel rather than the overall pattern (Ashworth and Lewin, 2012).

At the opposite corner of Figure 7 is a subset of coarse-bed reaches that I have labelled as 'torrents'. These are the steep and shallow end-members of the general class of coarse-bed channels, with gradients exceeding 0.01 (in some cases >0.1) and beds containing boulders (D_{50} usually in the 50–100 mm range). They are always small, with bankfull discharge usually below 10 $m^3\ s^{-1}$ and bankfull depth no more than 1 m, and thus have very low relative submergence ($d/D_{50} < 10$). This is the default channel type in the mountain headwaters of many river systems (Church, 2013). The larger clasts protrude high into the flow even at high discharges, and above the water surface at low discharges, and consequently affect the flow structure. The vertical velocity profile is non-logarithmic and spatially variable, and flow resistance is very high at low discharge. It decreases markedly as discharge increases (Figure 1B), giving a distinctive at-a-station hydraulic geometry in which velocity increases faster than depth. Bankfull Shields numbers are often high, as can be seen in Figure 7, but the critical Shields number for significant entrainment of bed material is also high, particularly at slopes of order 0.1 rather than 0.01 (Figure 2). Phillips and Jerolmack (2019) argued that torrents are usually threshold channels for this reason, but this may depend on sediment supply. Pfeiffer *et al.* (2017) found that estimated θ_{bf}/θ_c ratios in headwater streams near the US west coast, a tectonically young region with high sediment supply and little channel armouring, averaged about 2, whereas those in the Rocky Mountains and east coast regions were close to threshold. Irrespective of this, the larger clasts in torrents are typically immobile for long periods, with bedload transport restricted to what is entrained from finer patches and occurring at a lower rate than is predicted by standard formulae (Yager *et al.*, 2007). When large clasts do move in major floods, their size relative to channel width can lead to jamming (Church and Zimmerman, 2007) and the formation of organized stone structures. Boulder steps are generally present at gradients above about 0.04 (Montgomery and Buffington, 1997).

Conclusions

Invariances and simple power-law or logarithmic scalings are often assumed to apply to all rivers, and some of them are good approximations over a wide range of conditions, but they all start to break down in one or other part of the continuum of river size, gradient, and bed material. Some departures from scale invariance relate to changes in the relative importance of opposing forces, as in the case of settling velocity.

Inspection of a large compilation of data from reaches in all parts of the continuum supports the existence of two main types (gravel/boulder bed and sand bed) and the relative scarcity of reaches with bed D_{50} in the transitional 1–10 mm range. Most of the suggested reasons for this scarcity involve consideration of the size distribution (often bimodal), not just its median, and some involve departures from simple scaling in the entrainment and suspension thresholds. Scaling considerations support the assumption that coarse-bed reaches have near-threshold bedload transport regimes whereas sand-bed reaches have mixed or suspension-dominated regimes. Bankfull Shields numbers range substantially within each type but have very different characteristic values.

Both types of river have a distinctive end-member subtype whose existence is related to scaling considerations. Very large ('mega') rivers all have very low gradients and bed D_{50} in the medium/fine sand range. They are distinguished from smaller sand-bed rivers by transport almost entirely in suspension during high flow, weaker secondary circulation, and particularly high backwater lengths. Very steep shallow 'torrents' with cobble/boulder beds have distinctively high flow resistance and entrainment threshold, as well as distinctive within-reach morphologies.

Bankfull channel dimensions follow simple power-law scaling with discharge, but the relations for coarse and fine-bed channels are slightly different.

There is considerable scatter around the flow resistance, transport rate, and hydraulic geometry scaling relations. Much of this scatter relates to the limitations of quantifying boundary sediment by bed D_{50} without considering gravel structures, sand bedforms, and bank material.

Acknowledgements—I thank Mike Church for reading the first draft of this review and making useful suggestions, and two anonymous reviewers for their thoughtful and constructive comments on the submitted manuscript.

Data Availability Statement

No new data were collected for or created in this paper. See the online Supporting Information for existing sources that were used.

Conflict of Interest

The author declares no conflict of interest.

References

Aberle J, Smart GM. 2003. The influence of roughness structure on flow resistance on steep slopes. *Journal of Hydraulic Research* **41**: 259–269.

Ackers P, Charlton FG. 1970. Slope and resistance of small meandering channels. *Proceedings of the Institute of Civil Engineers* **47**: 349–370.

Ancey C. 2020. Bedload transport: a walk between randomness and determinism. Part 1. The state of the art. *Journal of Hydraulic Research* **58**: 1–17.

Andrews ED. 1984. Bed-material entrainment and hydraulic geometry of gravel-bed channels in Colorado. *Geological Society of America Bulletin* **95**: 371–378.

Armanini A, Gregoretti C. 2005. Incipient sediment motion at high slopes in uniform flow condition. *Water Resources Research* **41**: W12431. https://doi.org/10.1029/2005WR004001

Ashmore PE. 1991. How do gravel-bed rivers braid? *Canadian Journal of Earth Sciences* **28**: 326–341.

Ashworth PJ, Ferguson RI. 1989. Size-selective entrainment of bed load in gravel bed streams. *Water Resources Research* **25**: 627–634.

Ashworth PJ, Lewin J. 2012. How do big rivers come to be different? *Earth-Science Reviews* **114**: 84–107.

Bagnold RA. 1966. An approach to the sediment transport problem from general physics. *US Geological Survey Professional Papers* **422-I**: 231–291.

Bagnold RA. 1977. Bedload transport by natural rivers. *Water Resources Research* **13**: 303–312.

Barry JJ, Buffington JM, King JG. 2004. A general power equation for predicting bed load transport rates in gravel bed rivers. *Water Resources Research* **40**: W10401. https://doi.org/10.1029/2004WR003190

Benson E. 2020. Random river: Luna Leopold and the promise of chance in fluvial geomorphology. *Journal of Historical Geography* **67**: 14–23.

Blench T. 1969. *Mobile-Bed Fluviology; A Regime Theory Treatment of Canals and Rivers for Engineers and Hydrologists*. University of Alberta Press: Edmonton.

Blom A, Arkesteljn L, Chavarrias V, Viparelli E. 2017a. The equilibrium alluvial river under variable flow and its channel-forming discharge. *Journal of Geophysical Research – Earth Surface* **122**: 1924–1948.

Blom A, Chavarrias V, Ferguson RI, Viparelli E. 2017b. Advance, retreat, and halt of abrupt gravel–sand transitions in alluvial rivers. *Geophysical Research Letters* **44**: 9751–9760.

Bray DI. 1982. Regime equations for gravel-bed rivers. In *Gravel-Bed Rivers*, Hey RD, Bathurst JC, Thorne CR (eds). Wiley: Chichester; 515–552.

Buffington JM, Montgomery DR. 1997. A systematic analysis of eight decades of incipient motion studies with special reference to gravel-bedded rivers. *Water Resources Research* **33**: 1993–2029.

Bunte K, Abt SR, Swingle KW, Cenderelli DA, Schneider JM. 2013. Critical Shields values in coarse-bedded steep streams. *Water Resources Research* **49**: 7427–7447.

Chang HH. 1988. *Fluvial Processes in River Engineering*. Wiley: New York.

Church M. 2006. Bed material transport and the morphology of alluvial river channels. *Annual Review of Earth and Planetary Science* **34**: 325–354. https://doi.org/10.1146/annurev.earth.33.092203.122721

Church M. 2013. Steep headwater channels. In *Treatise on Geomorphology*, Shroder J, Wohl E (eds). Academic Press: San Diego, CA; 528–549.

Church M, Ferguson RI. 2015. Morphodynamics: rivers beyond steady state. *Water Resources Research* **51**: 1883–1897.

Church M, Rood K. 1983. *Catalogue of Alluvial Channel Regime Data*. University of British Columbia: Vancouver data available at http://www.nced.umn.edu/

Church M, Zimmerman A. 2007. Form and stability of step-pool channels: research progress. *Water Resources Research* **43**: W03415. https://doi.org/10.1029/2006WR005037

Church M, Hassan MA, Wolcott JF. 1998. Stabilizing self-organized structures in gravel-bed stream channels: field and experimental observations. *Water Resources Research* **34**: 3169–3179.

Crosato A, Mosselman E. 2009. Simple physics-based predictor for the number of river bars and the transition between meandering and braiding. *Water Resources Research* **43**: W03424. https://doi.org/10.1029/2008WR007242

Dade WB, Friend PF. 1998. Grain-size, sediment-transport regime, and channel slope in alluvial rivers. *Journal of Geology* **106**: 661–675.

Dingman SL. 2009. *Fluvial Hydraulics*. Oxford University Press: Oxford.

Dunne KBJ, Jerolmack DJ. 2018. Evidence of, and a proposed explanation for, bimodal transport states in alluvial rivers. *Earth Surface Dynamics* **6**: 583–594.

Eaton BC. 2013. Hydraulic geometry: empirical investigations and theoretical approaches. In *Treatise on Geomorphology*, Shroder J, Wohl E (eds). Academic Press: San Diego, CA; 313–329.

Eaton BC, Church M. 2007. Predicting downstream hydraulic geometry: a test of rational regime theory. *Journal of Geophysical Research – Earth Surface* **112**: F03025. https://doi.org/10.1029/2006JF000724

Eaton BC, Millar RG. 2004. Optimal alluvial channel width under a bank stability constraint. *Geomorphology* **62**: 35–45.

Eaton BC, Church M, Millar RG. 2004. Rational regime model of alluvial channel morphology and response. *Earth Surface Processes and Landforms* **29**: 511–529.

Einstein HA. 1950. *The Bed-Load Function for Sediment Transport in Open Channel Flows*. Soil Conservation Service Technical Bulletin 1026. U.S. Department of Agriculture: Washington, D.C.

Engelund F. 1974. Flow and bed topography in channel bends. *Journal of the Hydraulic Division, ASCE* **100**: 1631–1648.

Engelund F, Hansen E. 1967. *A Monograph on Sediment Transport in Alluvial Streams*. Teknisk Forlag: Copenhagen.

Ferguson R. 2003. The missing dimension: effects of lateral variation on 1-D calculations of fluvial bedload transport. *Geomorphology* **56**: 1–14.

Ferguson R. 2007. Flow resistance equations for gravel- and boulder-bed streams. *Water Resources Research* **43**: W05427. https://doi.org/10.1029/2006WR005422

Ferguson R. 2010. Time to abandon the Manning equation? *Earth Surface Processes and Landforms* **35**: 1873–1876.

Ferguson RI. 2012. River channel slope, flow resistance, and gravel entrainment thresholds. *Water Resources Research* **48**: W05517. https://doi.org/10.1029/2011WR10850

Ferguson R. 2013. Reach-scale flow resistance. In *Treatise on Geomorphology*, Schroder J, Wohl E (eds). Elsevier: San Diego; 50–68.

Ferguson RI, Church M. 2004. A simple universal equation for grain settling velocity. *Journal of Sedimentary Research* **74**: 933–937.

Ferguson RI, Bloomer DJ, Church M. 2011. Evolution of an advancing gravel front: observations from Vedder Canal, British Columbia. *Earth Surface Processes and Landforms* **36**: 1172–1182.

Ferguson RI, Sharma BP, Hardy RJ, Hodge RA, Warburton J. 2017. Flow resistance and hydraulic geometry in contrasting reaches of a bedrock channel. *Water Resources Research* **53**: 2278–2293.

Frings RM. 2011. Sedimentary characteristics of the gravel–sand transition in the River Rhine. *Journal of Sedimentary Research* **81**: 52–63.

Frings RM, Kleinhans MG, Vollmer S. 2008. Discriminating between pore-filling load and bed-structure load: a new porosity-based method, exemplified for the river Rhine. *Sedimentology* **55**: 1571–1593.

Gimenez-Curto LA, Corniero Lera MA. 1996. Oscillating turbulent flow over very rough beds. *Journal of Geophysical Research – Oceans* **101**: 20745–20758.

Gran K, Paola C. 2001. Riparian vegetation control on braided stream dynamics. *Water Resources Research* **37**: 3275–3283.

Griffiths GA. 2003. Downstream hydraulic geometry and hydraulic similitude. *Water Resources Research* **39**: 1094. https://doi.org/10.1029/2002WR001485

Hallermeier RJ. 1981. Terminal settling velocity of commonly occurring sand grains. *Sedimentology* **28**: 859–865.

Hassan MA, Brayshaw D, Alila Y, Andrews E. 2014. Effective discharge in small formerly glaciated mountain streams of British Columbia: limitations and implications. *Water Resources Research* **50**: 4440–4458.

Henderson FM. 1961. Stability of alluvial channels. *Journal of the Hydraulics Division ASCE* **87**: 109–137.

Hey RD. 1979. Flow resistance in gravel-bed rivers. *Journal of the Hydraulics Division ASCE* **105**: 365–379.

Hey RD, Thorne CR. 1986. Stable channels with mobile gravel beds. *Journal of the Hydraulics Division ASCE* **112**: 671–689.

Hey RD, Bathurst JC, Thorne CR (eds). 1982. *Gravel-Bed Rivers*. Wiley: Chichester.

Hinton D, Hotchkiss RH, Cope M. 2018. Comparison of calibrated empirical and semi-empirical methods for bedload transport rate prediction in gravel bed streams. *Journal of Hydraulic Engineering* **144**: 04018038. https://doi.org/10.1061/(ASCE)HY.1943-7900.0001474

Howard AD. 1980. Thresholds in river regimes. In *Thresholds in Geomorphology*, Coates D, Vitek J (eds). Allen & Unwin: Boston; 227–258.

Inglis CC. 1947. Meanders and their bearing on river training. Institution of Civil Engineers Maritime and Waterways, paper 7.

Johnson JPL. 2014. A surface roughness model for predicting alluvial cover and bedload transport rate in bedrock channels. *Journal of Geophysical Research – Earth Surface* **119**: 2147–2173. https://doi.org/10.1029/2013JF003000

Johnson JPL. 2016. Gravel threshold of motion: a state function of sediment transport disequilibrium? *Earth Surface Dynamics* **4**: 685–703.

Jones RAL. 2004. *Soft Machines*. Oxford University Press: Oxford.

Keulegan GH. 1938. Laws of turbulent flow in open channels. *Journal of Research National Bureau of Standards* **21**: 707–741.

Kleinhans MG. 2005. Flow discharge and sediment transport models for estimating a minimum timescale of hydrological activity and delta formation on Mars. *Journal of Geophysical Research – Planets* **110**: E12003. https://doi.org/10.2029/2005JE002521

Kleinhans MG. 2010. Sorting out river channel patterns. *Progress in Physical Geography* **34**: 287–326.

Kleinhans MG, van den Berg JH. 2011. River channel and bar patterns explained and predicted by an empirical and a physics-based method. *Earth Surface Processes and Landforms* **36**: 721–738.

Kleinhans MG, Braudrick C, van Dijk WM, van de Lageweg WI, Teske R, van Oorschot M. 2015. Swiftness of biomorphodynamics in Lilliput- to giant-sized rivers and deltas. *Geomorphology* **224**: 56–73.

Kodama Y. 1994. Downstream changes in the lithology and grain-size of fluvial gravels, the Watarase river, Japan – evidence of the role of abrasion in downstream fining. *Journal of Sedimentary Petrology A* **64**: 68–75.

Lacey G. 1930. Stable channels in alluvium. *Proceedings of the Institute of Civil Engineers* **229**: 259–292.

Lamb MP, Venditti JG. 2016. The grain size gap and abrupt gravel–sand transitions in rivers due to suspension fallout. *Geophysical Research Letters* **43**: 3777–3785.

Lamb MP, Dietrich WE, Venditti JG. 2008. Is the critical Shields stress for incipient sediment motion dependent on channel-bed slope? *Journal of Geophysical Research – Earth Surface* **113**: F02008.

Latrubesse EM. 2008. Patterns of anabranching channels: the ultimate end-member adjustment of mega rivers. *Geomorphology* **101**: 130–145.

Latrubesse EM, Stevaux JC, Sinha R. 2005. Tropical rivers. *Geomorphology* **70**: 187–206.

Lawrence DSL. 1997. Macroscale surface roughness and frictional resistance in overland flow. *Earth Surface Processes and Landforms* **22**: 365–382.

Lee J-S, Julien PY. 2006. Downstream hydraulic geometry of natural channels. *Journal of Hydraulic Engineering* **132**: 146–153.

Leopold LB, Maddock T. 1953. Hydraulic geometry of stream channels and some physiographic implications. *U.S. Geological Survey Professional Papers* **272**: 1–57.

Leopold LB, Wolman MG. 1960. River meanders. *Geological Society of America Bulletin* **71**: 769–794.

Leopold LB, Bagnold RA, Wolman MG, Brush LM. 1960. Flow resistance in sinuous and irregular channels. *U.S. Geological Survey Professional Papers* **282D**: 111–134.

Li C, Czapiga MJ, Eke EC, Viparelli E, Parker G. 2015. Variable Shields number model for river bankfull geometry: bankfull shear velocity is viscosity-dependent but grain size-independent. *Journal of Hydraulic Research* **53**: 36–48.

Ma H, Nittrouer JA, Wu B, Lamb MP, Zhang Y, Mohrig D, Fu X, Naito K, Wang Y, Moodie AJ, Wang G, Hu C, Parker G. 2020. Universal relation with regime transition for sediment transport in fine-grained rivers. *Proceedings of National Academy of Sciences* **117**: 171–176.

MacKenzie LG, Eaton BC, Church M. 2018. Breaking from the average: why large grains matter in gravel-bed streams. *Earth Surface Processes and Landforms* **43**: 3190–3196.

Mertes LAK, Daniel DL, Melack JM, Nelson B, Martinelli LA, Forsberg BR. 1995. Spatial patterns of hydrology, geomorphology, and vegetation on the floodplain of the Amazon River in Brazil from a remote-sensing perspective. *Geomorphology* **13**: 215–232.

Meyer-Peter E, Müller R. 1948. Formulas for bed-load transport. In *Proceedings of the 2nd Congress*. International Association of Hydraulic Research: Stockholm; 39–64.

Millar RG. 2005. Theoretical regime equations for mobile gravel-bed rivers with stable banks. *Geomorphology* **64**: 207–220.

Miller MC, McCave IN, Komar PD. 1977. Threshold of sediment motion under unidirectional currents. *Sedimentology* **24**: 507–527.

Montgomery DR, Buffington JM. 1997. Channel-reach morphology in mountain drainage basins. *Geological Society of America Bulletin* **109**: 596–611.

Mueller ER, Pitlick J, Nelson JM. 2005. Variation in the reference Shields stress for bed load transport in gravel-bed streams and rivers. *Water Resources Research* **41**: W04006. https://doi.org/10.1029/2004WR003692

Nicholas A. 2013. Morphodynamic diversity of the world's largest rivers. *Geology* **41**: 475–478.

Nikora V, Goring D, McEwan I, Griffiths G. 2001. Spatially averaged open-channel flow over rough bed. *Journal of Hydraulic Engineering* **127**: 123–133.

Nino Y, Lopez F, Garcia M. 2003. Threshold for particle entrainment into suspension. *Sedimentology* **50**: 247–263.

Nitsche M, Rickenmann D, Turowski JM, Badoux A, Kirchner JW. 2011. Evaluation of bedload transport predictions using flow resistance equations to account for macro-roughness in steep mountain streams. *Water Resources Research* **47**: W08513. https://doi.org/10.1029/2011WR010645

Nitsche M, Rickenmann D, Kirchner JW, Turowski JM, Badoux A. 2012. Macroroughness and variations in reach-averaged flow resistance in steep mountain streams. *Water Resources Research* **48**: W12518. https://doi.org/10.1029/2012WR012091

Nittrouer JA. 2013. Backwater hydrodynamics and sediment transport in the lowermost Mississippi River delta: implications for the development of fluvial-deltaic landforms in a large lowland river. *International Association of Hydrological Science Publications* **258**: 48–61.

Palucis M, Lamb M. 2017. What controls channel form in steep mountain streams? *Geophysical Research Letters* **44**: 7245–7255.

Parker G. 1978. Self-formed straight rivers with equilibrium banks and mobile bed. Part 2. The gravel-bed river. *Journal of Fluid Mechanics* **89**: 127–146.

Parker G. 1979. Hydraulic geometry of active gravel rivers. *Journal of the Hydraulics Division ASCE* **105**: 1185–1201.

Parker G. 1990. Surface-based bedload transport relation for gravel rivers. *Journal of Hydraulic Research* **28**: 417–436.

Parker G. 1991. Selective sorting and abrasion of river gravel. II. Applications. *Journal of Hydraulics Division ASCE* **117**: 150–171.

Parker G, Toro-Escobar CM, Ramey M, Beck S. 2003. The effect of floodwater extraction on the morphology of mountain streams. *Journal of Hydraulic Engineering* **129**: 885–895.

Parker G, Wilcock PR, Paola C, Dietrich WE, Pitlick J. 2007. Physical basis for quasi-universal relations describing bankfull hydraulic geometry of single-thread gravel bed rivers. *Journal of Geophysical Research – Earth Surface* **112**: F04005.

Pfeiffer AM, Finnegan NJ, Willenbring JK. 2017. Sediment supply controls equilibrium channel geometry in gravel rivers. *Proceedings of the National Academy of Sciences USA* **114**: 3346–3351.

Phillips CB, Jerolmack DJ. 2019. Bankfull transport capacity and the threshold of motion in coarse-grained rivers. *Water Resources Research* **55**: 11316–11330.

Phillips JD, Slattery MC. 2007. Downstream trends in discharge, slope and stream power in a coastal plain river. *Journal of Hydrology* **334**: 290–303.

Powell DM. 2015. Flow resistance in gravel-bed rivers: progress in research. *Earth-Science Reviews* **136**: 301–338.

Radoane M, Radoane N, Dumitriu D, Miclaus C. 2008. Downstream variation in bed sediment size along the East Carpathian rivers: evidence of the role of sediment sources. *Earth Surface Processes and Landforms* **33**: 674–694.

Recking A. 2009. Theoretical development on the effects of changing flow hydraulics on incipient bed motion. *Water Resources Research* **45**: W04401. https://doi.org/10.1029/2008WR006826

Recking A. 2010. A comparison between flume and field based bed load transport data and consequences for surface-based bed load transport prediction. *Water Resources Research* **46**: W03518. https://doi.org/10.1029/2009WR008007

Recking A. 2013. Simple method for calculating reach-averaged bedload transport. *Journal of Hydraulic Engineering* **139**: 70–75.

Recking A, Piton G, Vazquez-Tarrio D, Parker G. 2016. Quantifying the morphological print of bedload transport. *Earth Surface Processes and Landforms* **41**: 809–822.

Reid I, Frostick LE, Layman JT. 1985. The incidence and nature of bedload transport during flood flows in coarse-grained alluvial channels. *Earth Surface Processes and Landforms* **10**: 33–44.

Rickenmann D. 1991. Hyperconcentrated flow and sediment transport at steep slopes. *Journal of Hydraulic Engineering* **117**: 1419–1439.
Rickenmann D. 2001. Comparison of bed load transport in torrents and gravel bed streams. *Water Resources Research* **37**: 3295–3305.
Rickenmann D, Recking A. 2011. Evaluation of flow resistance equations using a large field data base. *Water Resources Research* **47**: W07538. https://doi.org/10.1029/2006WR005422
Rozovskii IL. 1957. Flow of water in bends of open channels. Academy of Sciences of the Ukrainian SSR: Kiev (translated from the Russian by the Israel Program for Scientific Translations, Jerusalem, 1961).
Samuels PG. 1989. Backwater lengths in rivers. *Proceedings of the Institute of Civil Engineers* **87**: 571–582.
Schoklitsch A. 1934. Der Geschiebetrieb und die Geschiebekraft. *Wasserkraft Wasserwirt* **29**: 37–43.
Shaw J, Kellerhals R. 1982. *The Composition of Recent Alluvial Gravels in Alberta River Beds*. Alberta Research Council: Alberta.
Shields A. 1936. *Anwendung der Aehnlichkeitsmechanik und der Turbulenzforschung auf die Geschiebebewegung [Application of Similarity Mechanics and Turbulence Research on Shear Flow]*. Preußische Versuchsanstalt für Wasserbau: Berlin.
Simons DB, Albertson ML. 1960. Uniform water-conveyance channels in alluvial material. *Journal of the Hydraulics Division ASCE* **86**: 33–71.
Singer MB. 2008. Downstream patterns of bed material grain size in a large, lowland alluvial river subject to low sediment supply. *Water Resources Research* **44**(12): W12202. https://doi.org/10.1029/2008WR007183
Smith GHS, Ferguson RI. 1995. The gravel to sand transition along river channels. *Journal of Sedimentary Research* **65A**: 423–430.
Smith GHS, Ashworth PJ, Best JL, Woodward J, Simpson CJ. 2005. The morphology and facies of sandy braided rivers: some considerations of scale invariance. *International Association of Sedimentologists Special Publications* **35**: 145–158.
Strickler A. 1923. *Beitrage zur Frage der Geschwindigkeitsformel und der Rauhigkeitszahlen für Ströme, kanäle, und geschlossene Laitungen. Mitteilungen des Amtes für Wasserwirtschaft*. Eidgenössisches Departement des Innern: Bern.
Struiksma N. 1985. Prediction of 2-D bed topography in rivers. *Journal of Hydraulic Engineering ASCE* **111**: 1169–1182.
Tooth S. 2000. Process, form and change in dryland rivers: a review of recent research. *Earth-Science Reviews* **51**: 67–107.
Trampush SM, Huzurbazar S, McElroy B. 2014. Empirical assessment of theory for bankfull characteristics of alluvial channels. *Water Resources Research* **50**: 9211–9220.
Trigg MA, Wilson MD, Bates PD, Horritt MS, Alsdorf DE, Forsberg BR, Vega MC. 2009. Amazon flood wave hydraulics. *Journal of Hydrology* **374**: 92–105.
Tubino M. 1991. Growth of alternate bars in unsteady flow. *Water Resources Research* **27**: 37–52.
van Rijn LC. 1984. Sediment transport. Part II: Suspended load transport. *Journal of Hydraulic Engineering* **110**: 1613–1641.
Venditti JG, Church M. 2014. Morphology and controls on the position of a gravel–sand transition: Fraser River, British Columbia. *Journal of Geophysical Research – Earth Surface* **119**: 1959–1976.
Wathen SJ, Ferguson RI, Hoey TB, Werritty A. 1995. Unequal mobility of gravel and sand in weakly bimodal river sediments. *Water Resources Research* **31**: 2087–2096.
Wilcock PR, McArdell BW. 1997. Partial transport of a sand/gravel sediment. *Water Resources Research* **33**: 235–245.
Wilcock PR, Kenworthy ST, Crowe JC. 2001. Experimental study of the transport of mixed sand and gravel. *Water Resources Research* **37**: 3349–3358.
Wilkerson GV, Parker G. 2011. Physical basis for quasi-universal relationships describing bankfull hydraulic geometry of sand-bed rivers. *Journal of Hydraulic Engineering* **137**: 739–753.
Wolcott J. 1988. Nonfluvial control of bimodal grain-size distributions in river-bed gravels. *Journal of Sedimentary Petrology* **58**: 979–984.
Xu J-X. 2004. Comparison of hydraulic geometry between sand- and gravel-bed rivers in relation to channel pattern discrimination. *Earth Surface Processes and Landforms* **29**: 645–657.
Yager EM, Kirchner JW, Dietrich WE. 2007. Calculating bed load transport in steep boulder bed channels. *Water Resources Research* **43**: W07418. https://doi.org/10.1029/2006WR005432
Yager EM, Venditti JG, Smith HJ, Schmeekle MW. 2018. The trouble with shear stress. *Geomorphology* **323**: 41–50.
Yatsu E. 1957. On the discontinuity of grain-size frequency distribution of fluvial deposits and its geomorphological significance. *Proceedings of the International Geophysical Union Regional Conference, Tokyo, Japan*; 224–237.

Supporting Information

Additional supporting information may be found online in the Supporting Information section at the end of the article.

Figures 1A, 5 and 7 are based on a new compilation of previously published bankfull measurements; see below.
Figure 1B uses data analysed by Rickenmann and Recking (2011); I obtained them from A. Recking (personal communication, 2018) but they are available at https://www.bedloadweb.com//.
Figure 2 plots data available in sources tabulated in Ferguson (2012). Figure 3A uses data tabulated in Hallermeier (1981) and Ferguson and Church (2004).
Figure 4A uses data from Recking *et al*. (2016), available at https://onlinelibrary-wiley-com.ezphost.dur.ac.uk/action/downloadSupplement?doi=10.1002%2Fesp.3869&file=esp3869-sup-0001-SI.zip.
Figure 4B uses data from Ma *et al*. (2020), available at https://figshare.com/articles/Database_of_Bed_Material_Load_Transport_in_Flumes_and_Rivers_with_Fine-grained_Beds/10060241.